ijlpr 2023; doi 10.22376/ijlpr.2023.13.2.P127-P134

International Journal of Life science and Pharma Research

ISSN 2250-0480

Study of Synthesis and Characterization of Pure Cus and Cufes Nanoparticles by Hydrothermal Method

L. Thilagavathi[a], Dr.M. Venkatachalam[b], Dr.M. Saroja[b] and Dr.T.S. Senthil[c]

[a, b] *Department of Electronics, Erode Arts and Science College, Erode, India -638 009.*

[c] *Department of Physics, Erode Sengunthar Engineering College, Perundurai, India -638057*

Abstract: Copper-based material has good electrical and optical properties but is not only physical properties and also good in antibacterial applications. Nano-structured CuS has potential value on high photocatalytic activity because of their suitable band gap and catalytic ability. CuS NP hydrogels had both adjustable physical properties and good injectable self-healing characteristics and excellent functionalities, concurrently including hemostatic ability, bacteria-killing capability, and cell migration and proliferation promotion. *In vivo* wound, healing, and histomorphological examinations of immunofluorescence staining in a mouse full-thickness wound model demonstrated good acceleration effects of these hydrogels for infected wound healing. A novel Chalcopyrite CuFeS nanocrystals are used as a Fenton reagent to degrade organic dyes without any additional source efficiently. Subsequently, the $CuFeS_2$ nanocrystals/ biomass composite degradation column is made, continually degrading organic dyes. This paper demonstrates a comparative study of the synthesis and characterization of pure CuS and CuFeS nanoparticles using copper chloride, thiourea, ferric chloride and water solvent by straightforward hydrothermal methods. The synthesized material was characterized by an X-ray diffraction (XRD), Scanning Electron Microscope (SEM), and Energy Dispersive X-ray spectrum (EDAX) techniques employed to study the nanostructure properties of the prepared sample. Crystallite size was determined by the Debye-Scherrer formula and found to be 15.5 nm and 20.55 nm, respectively. The EDAX spectrum showed a clear peak of present elements. An SEM image shows the morphology of the nanostructures. Optical analysis was done with UV and FTIR techniques. The pure CuS and CuFeS synthesized Tauc Relation and calculated nanomaterials bandgap came out to be 4.6eV and 4.4 eV, respectively.

Keywords: CuS, CuFeS, hydrothermal, characterization, antibacterial.

***Corresponding Author**

L. Thilagavathi , Department of Electronics, Erode Arts and Science College, Erode, India -638 009.

Received On 4 October, 2022

Revised On 23 December, 2022

Accepted On 13 January, 2023

Published On 1 March, 2023

Funding This research did not receive any specific grant from any funding agencies in the public, commercial or not for profit sectors.

Citation L. Thilagavathi, Dr.M. Venkatachalam, Dr.M. Saroja and Dr.T.S. Senthil , Study of Synthesis and Characterization of Pure Cus and Cufes Nanoparticles by Hydrothermal Method.(2023).Int. J. Life Sci. Pharma Res.13(2), P127-P134 http://dx.doi.org/10.22376/ijlpr.2023.13.2.P127-P134

1. INTRODUCTION

High-performance information-rich energy-conscious upper electrical energy storage devices are important today for supplying electricity to mobile information-rich copper and energy-conscious society. Copper sulfide has attracted great attention because of not only its tremendous optical and electrical properties but their utility in various operational settings such as semiconductor layers allowing for enhancement of solar–to–electric energy in portal remote sensing and radar, but also due to their different applications such as solar cells, nano medicine, nano switches, a major focus of optical filter and catalysts[1]. The use of CuS for degrading environmental pollutants has stimulated interest due to its high efficiency, non-toxic nature, and low cost. In particular, nano-structured CuS has potential value in high photocatalytic activity because of their suitable band gap and catalytic ability. CuS NP hydrogels had both adjustable physical properties and good injectable self-healing characteristics and excellent functionalities, concurrently including hemostatic ability, bacteria-killing capability, and cell migration and proliferation promotion. *In vivo* wound, healing, and histomorphological examinations of immunofluorescence staining in a mouse full-thickness wound model demonstrated good acceleration effects of these hydrogels for infected wound healing.[2] Therefore, these injectable self-healing CuS NP hydrogels which possess the abilities of hemostasis, antibacterial activity, and infected-wound healing promotion, exhibit great potential as *in situ* wound dressings [3]. A novel Chalcopyrite CuFeS nanocrystals are used as a Fenton reagent to degrade organic dyes without any additional source efficiently. Subsequently, the $CuFeS_2$ nanocrystals/ biomass composite degradation column is made, continually degrading organic dyes[4]. In the CuS, various morphologies of CuS like nanorods, nanoflakes, nanotubes, nanospheres, nanowires, nanoplatelets, flower-like structures, nanotubes and nanoribbons have been reported. Various preparatory routes have been reported, like microwave, co-precipitation, sol-gel, solvothermal/hydrothermal, chemical vapour deposition, template-assisted growth, and polyol method. Apart from these various techniques, a hydrothermal route is preferred. The hydrothermal method is the most appealing because it could be operable at less temperature with high efficiency and could be scaled up[5]. Copper sulfide CuS is used as a textile mordant, agricultural pesticide, water fungicide, feed additive and copper plating. Solar cells, super-ion conductors, photodetectors, Conductive electrodes, photothermal spectrum analysis conversion equipment, microwave shielding coating, radio wave absorbers, and infrared radiation polarizers for gas sensors.[6] Copper sulfide (I) is used as semiconductor and in photographic applications [7]Their applications also include use in solar cells, luminous paints, electrodes and certain varieties of solid lubricants [8]. copper (II) sulfide finds applications in solar cells, superionic conductors, photodetectors, electroconductive electrodes, photothermal conversion devices, microwave protective coating, active radio wave absorbers, gas sensors and radiation polarizers Infrared [9] Copper (II) sulfide finds the applications (photocatalytic degradation, cancer cell ablation, electrode material in lithium-ion and gas-cell batteries, field emission properties, super capacitor applications, photoelectrochemical performance of QDSCs, photocatalytic reduction of organic pollutants, bio- Electrochemical detection, enhanced PEC characteristics of pre-cut CuS film electrodes)[10] the nanoparticles of semiconductor copper sulphide (CuS NPs) was demonstrated for the visualization of photoacoustic tomographies with an laser at a wavelength of 1064 nm. [11]. In recent two decades, many researchers have published reports on preparing photocatalysts with nanometer-sized structures, e.g., nanoparticles, nanoplates, nanocubes, nanorods, nanotubes, or nanowires, as well as their photocatalytic activities, and the number of such reports is still increasing. Photocatalysts may be used for antifouling, antifogging, energy conservation and storage, deodorization, sterilization, self-cleaning, air purification, wastewater treatment, etc., and antibacterial activity. [12] When compared with other methods, photocatalysis is fast developing and gaining extra attention owing to its various advantages, such as low cost and high efficiency. Photocatalysis is a unique process for rectifying energy and environmental issues. Here, this work revealed the synthesis of pure CuS and CuFeS nanomaterial by hydrothermal method and investigated various properties.

2. MATERIALS AND METHODS

2.1 Pure CuS

Liang Shi et al. method was followed[13,] where, 2mmol of $CuCl_2$.2H2O was dissolved in 100ml mixed solution, which was formed by DI water, and 5 mmol thioureas were added to the above solution under 700 rpm magnetic stirring for 1 hour to achieve homogeneous mixing. The solution was formed and then transferred into a Teflon-lined stainless steel autoclave with a volume of 100 ml and heated at 1500 for 24 hours. The autoclave slowly cooled to room temperature. The achieved Precipitate was washed with DI water and then dried at 50°C for 5 hours. Finally, the Precipitate was transferred to a silica Crucible for annealing at 400°C for 1 hour and then retrieved after 24 hours & Cool at room temperature, and ground well to get fine Powder for further characterization.

2.2 CuFeS

Daxin Liang et al. method was followed[14] for the preparation of CuFeS. 5mmol of $CuCl_2$ 2H2O was dissolved in 50ml mixed solution, 1 mmol of $FeCl_2$ was dissolved in 50ml mixed solution, both of which were formed by DI water, and mixing 0.01 mol of Na_2S was dissolved in 50ml and adding PVP the above solution colour changes occurring after continuous stirring at 700 rpm for 4 hours it will become the previous colour. Due to continued stirring, a small foam was generated. The solution was formed and then transferred into a Teflon-lined stainless steel autoclave with a volume of 100 ml and heated at 1500 for 24 hours. The autoclave slowly cooled to room temperature. The achieved precipitate was washed with DI water and then dried at 50°C for 5 hours. Finally, the precipitate was transferred to a silica Crucible for annealing at 400°C for 1 hour and then retrieved after 24 hours & Cool at room temperature, and ground well to get fine Powder for further characterization.

2.3 Structural analysis (XRD).[15]

The structural analysis was performed by using an X-ray diffractometer (Panalytical Netherland, x-pert3 powder). The X-ray generator operated at 45 kV and 30 mA. The Scanning regions of the diffraction angle (2θ) were 5-890, and Cu kα radiation was used to collect the spectrum. The XRD pattern of CuS and CuFeS nano-structures is shown below which can be indexed to Rhombohedral CuS and Hexagonal CuFeS structures. FESEM Analysis[16] The sample morphology was observed by Field Emission Scanning electron microscope (FESEM, Carl Zeiss microscopy Pvt. Ltd. UK). The size and

morphology of the CuS nanoparticles were observed by FE-SEM (SIGMA WITH GEMINI COLUMN, CARL ZEISS, USA). The nanoparticles samples were placed on an aluminium stud with double-sided conductive tape and coated with gold for 1 min in a vacuum by sputtering coating (using Au and Pd) with a resolution of 1.5nm to visualize under FE-SEM.[22] FESEM images of the CuS & CuFeS nanostructures are shown in figures 2 a and b with different magnifications.

2.4 *EDAX Analysis:*[17]

The energy-dispersive X-ray spectroscopy performed the elemental analysis. EDAX measurements were taken (Nano XFlash Detector, BRUKER, GERMAN) for elemental analysis through the point/area/ line scan and mapping. (EDX) and the spectrum is shown m Fig 3(a) and (b).

2.5 *UV Spectrophotometer Analysis*[18]

A UV-visible double beam spectrometer performs a UV-visible Spectrum analysis to characterize the optical properties. First, a very small sample was dissolved in the water. Then, the solution was sonicated in an ultrasonic bath for 10-15 minutes to obtain the uniform dispersion absorption spectrum in the wavelength range from 200 to 800 nm.

2.6 *FTIR Analysis*

FTIR analysis was carried out, responsible for reducing copper ions with the spectral range of 400-4000 cm^{-1}. The sample was exposed to IR Radiation in the KBr pellet form. [23] The pellet is made by mixing a very small amount of the sample into potassium bromide (KBr). Next, the mixture is grind properly for uniform sample distribution into the kBr base. Finally, the grinded mixture is pressed with a hydraulic press, applying a pressure of ~7 to 8 tons. The pure CuS Spectrum is acquired in the range 3330-641 and has a resolution of 2cm-1. The pure CuFeS Spectrum is acquired in the range 1100-610 and has a resolution of $2cm^{-1}$.

3. RESULTS AND DISCUSSION

Table 1: ***Structural analysis (XRD).***

Compound Name	Chemical Formula	PDF#	Score
Copper Sulfide	Cu1.8375 S	23-0962	36
Copper Iron Sulfide	Cu3.38 Fe0.62 S4	16-159	26

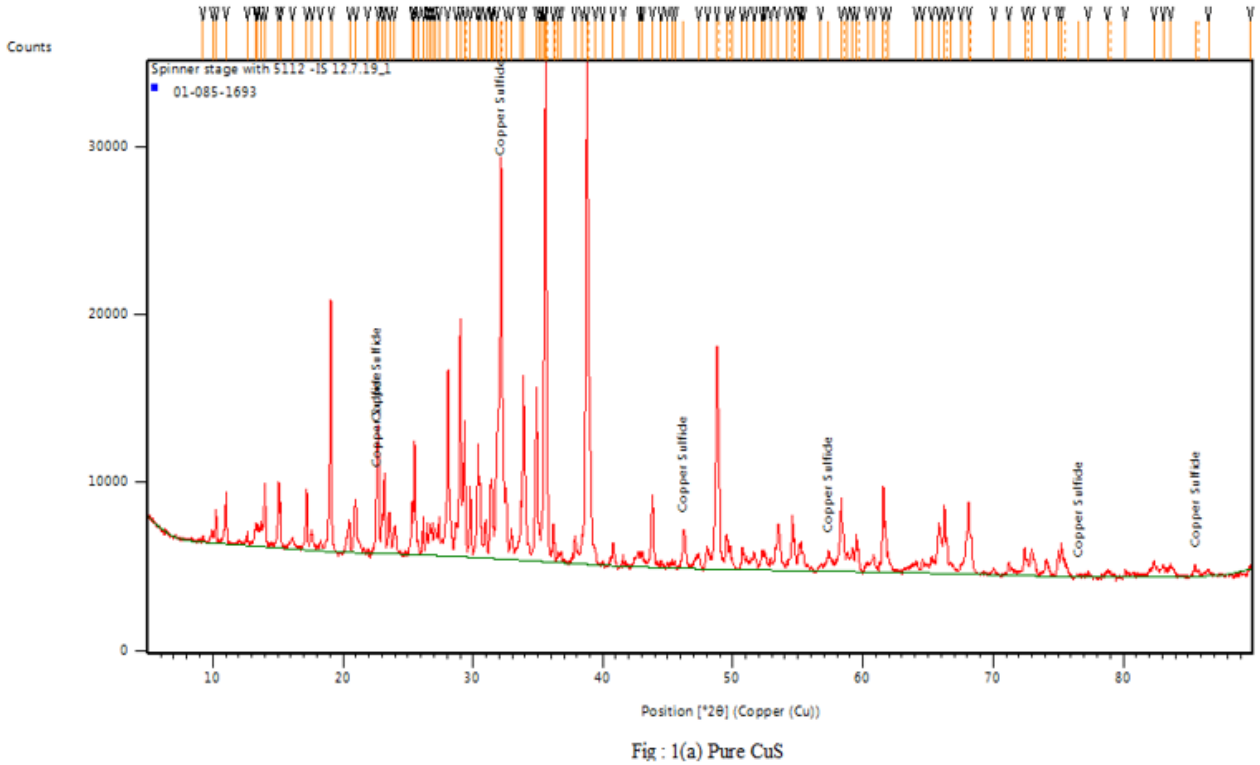

Fig : 1(a) Pure CuS

Fig :1 (a) XRD pattern for pure CuS.

In the XRD pattern of CuS (Fig. 1(a)), the three major peaks are in the 2θ values of 22.675^0,22.738^0, and 32.163^0, respectively.

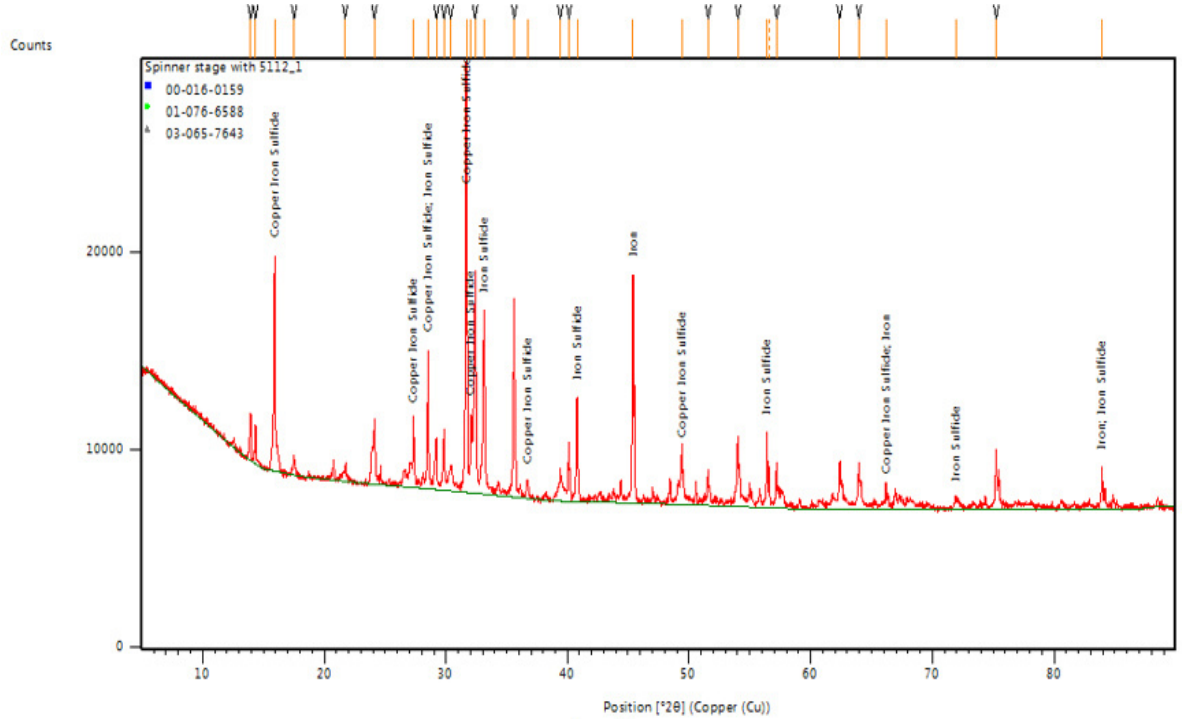

Fig :1 (b) CuFeS

Fig:1(b) XRD pattern for CuFeS

In the XRD pattern CuFeS, the three major peaks are seen in the 2θ values of 15.927°, 31.669°, and 32.422° respectively. The average particle can be calculated from the XRD Pattern using the well-known Debye - Scherrer formula given in the below equation (khan et al., 2013).

$$D = \frac{k\lambda}{\beta \cos\theta}$$

Where k → shape factor, β → Full Width of Half Maximum (FWHM) of the highest peak in radiation. λ= 1.540598 Å. Then the calculated particle size in CuS: D=15.4nm and CuFeS: D=20.55nm, respectively. The XRD pattern is shown in Fig.1 (a) compared with the standard pattern 23-0962, confirming the Rhombohedra crystalline of $Cu_{1.8}S$. The intensive peaks of the spectrum match with the characteristic pattern of diffraction for CuS, at 2θ values of 22.67°, 22.73°, and 32.16° respectively. And Fig.1(b) compared with the standard pattern number 16-159, confirming the Hexagonal crystalline of $Cu_{3.38}Fe_{0.62}S_4$. The intensive peaks of the spectrum match with the characteristic pattern of diffraction for CuFeS, at 2θ values of 15.927°, 31.669°, and 32.422° respectively.

3.1. FESEM analysis

The FESEM images reveal CuS nanoparticles are distributed non-uniformly with a somewhat agglomeration hexagonal shape, and similarly, the CuFeS nanoparticles were observed with a smooth surface and well-dispersed.

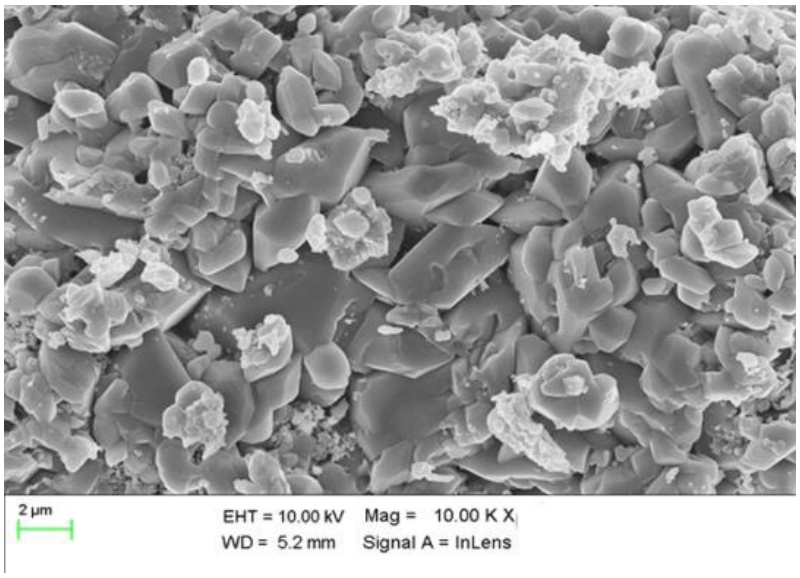

Fig 2(a): Pure CuS

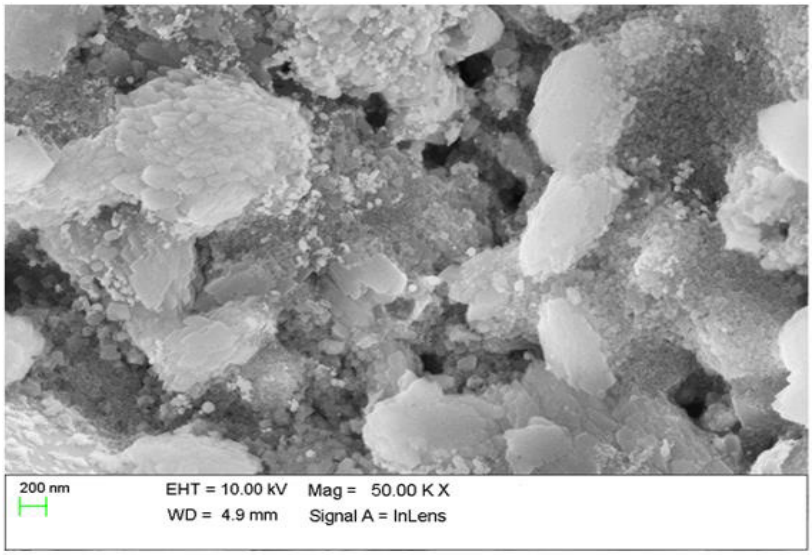

Fig 2(b): CuFeS

3.2. EDAX Analysis

The EDS Spectrum Confirms the Presence of Copper (Cu), sulfur (S), and Iron (Fe) in the Samples.

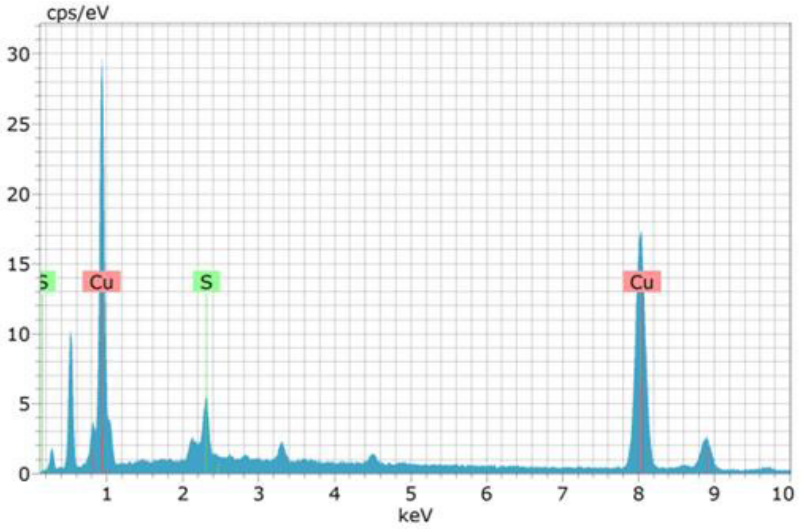

Fig 3(a): Pure CuS

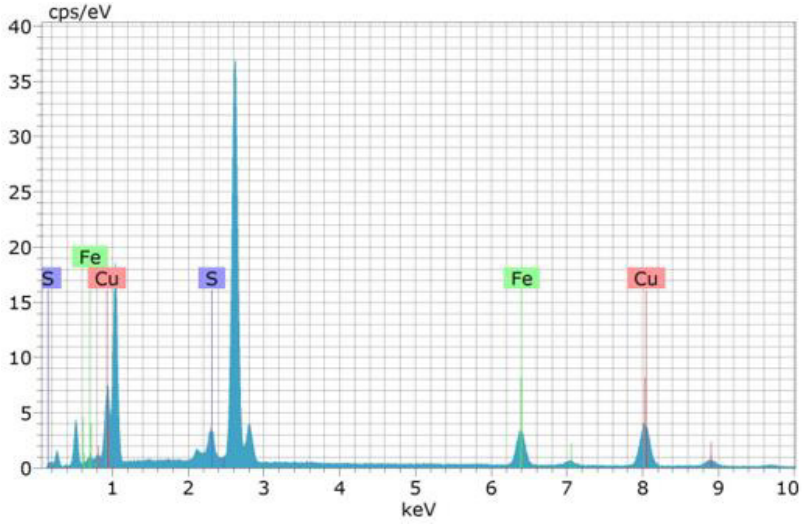

Fig 3(b) : CuFeS

The quantitative analysis of the elements in the CuS & CuFeS nanostructures and shown below.

Table: 2.1 Pure CuS		
Element	Wt %	At %
Copper	96.03	92.42
Sulfur	3.97	7.58

Table: 2.2 CuFeS		
Element	Wt %	At %
Copper	67.74	61.05
Iron	24.55	25.18
Sulfur	7.71	13.77

EDAX spectrum of the synthesized CuS nanoparticles. The signal peaks are strong for the copper atom at 0.9 and 8.1 keV and the sulfur atom at 2.3 keV. It was found that 96.03% of the copper weight was in the nanoparticles, but the remaining 3.97% was sulfur. Similarly, CuFeS, the strongest signal energy peaks for the copper atom 0.9 and 8.1 keV, iron atom 0.7 and 6.4 keV and sulfur 2.3 keV. The weight % of copper, iron and sulfur is 67.74%, 24.55% and 7.71%, respectively.

3.3. UV-Spectrophotometer analysis

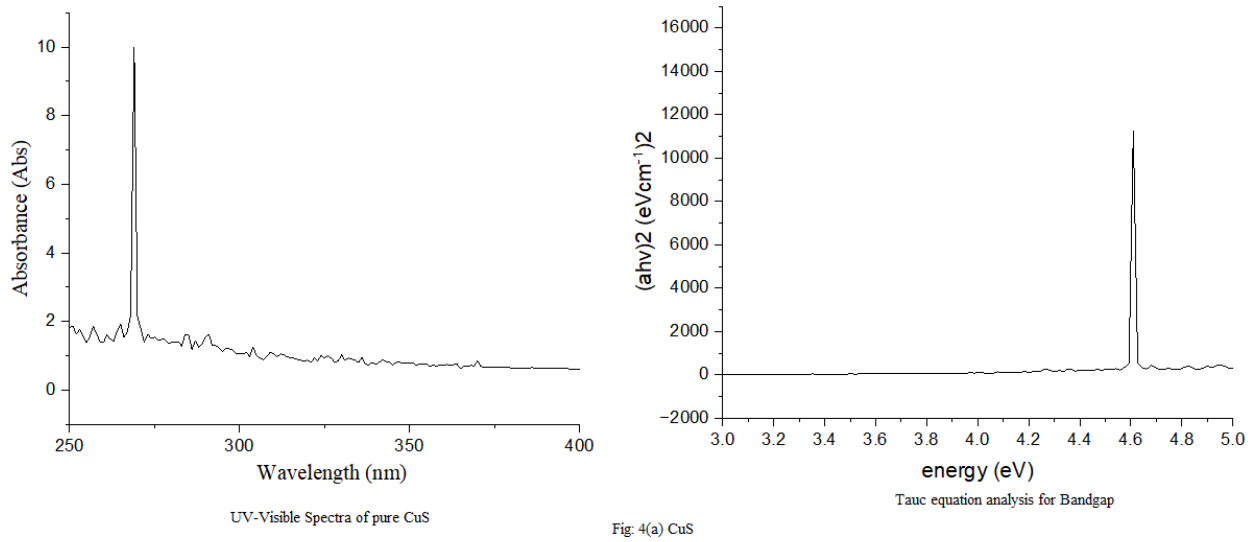

Fig 4 (a) : UV-Vis Spectra of pure CuS and Tauc equation analysis for Bandgap

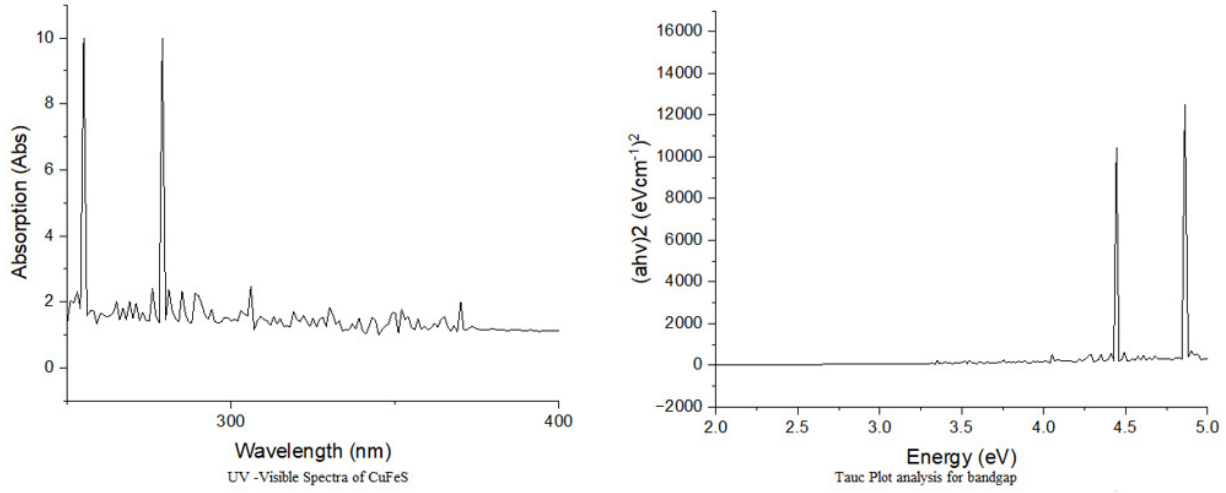

Fig: 4 (b) UV-Vis Spectra of CuFeS and Tauc equation analysis for Bandgap

The absorption, which Corresponds to electron excitation from the valence band to the Conduction band, can be used to determine the nature and value of the optical band gap. The relationship between the absorption coefficients (α) and the incident photon energy (hv) can be written as

$$\alpha h\nu = A(HV - Eg)^n$$

Where A, h,v and n→, Planck's Constant, incident light frequency, Eg →band gap of the material. According to the above equation, based on direct transition, the band gap of CuS is 4.6 eV and 4.4 eV for CuFeS, respectively. The optical properties of CuS and CuFeS nanoparticles have been studied using the absorption UV spectra recorded using a UV-Vis spectrometer. Figure 4(a), and (b) show the optical absorption spectra of the CuS nanoparticles. A significant decrease in the absorption below 400 nm wavelength can be attributed to light absorption caused by the excitation of electrons from the valence band to the conduction band of tungsten. It should also be noted that the films' absorption decreases with increased heat treatment temperatures. This may be due to the formation of larger particles on the surface of CuS and CuFeS nanoparticles, which causes light scattering.

3.4. FTIR analysis

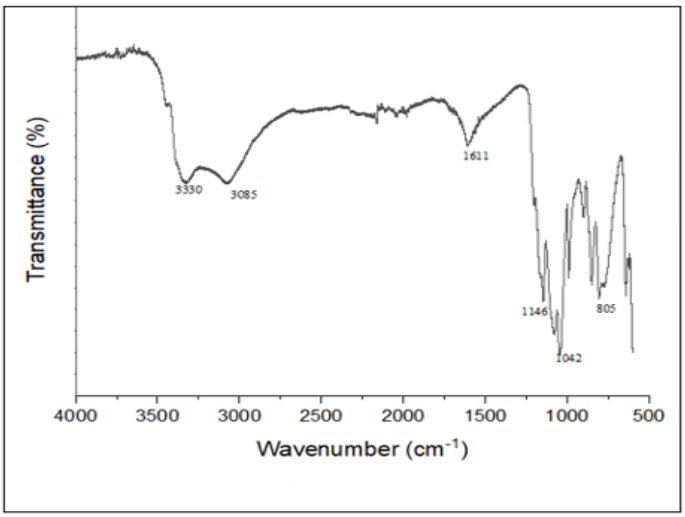

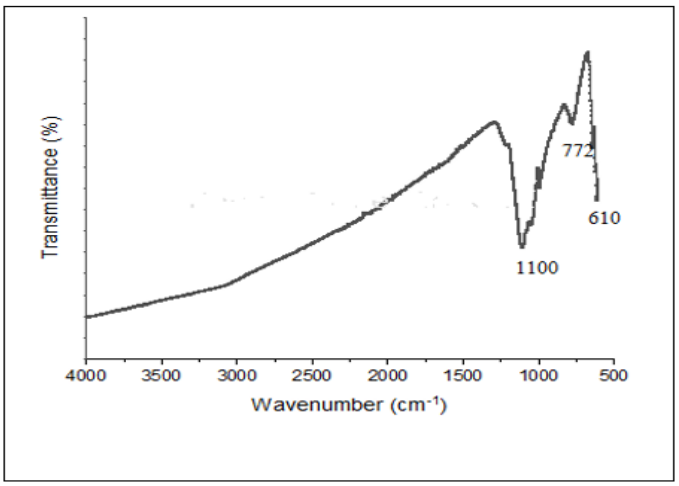

The characteristic band occurs for the vibration mode of water (OH group), indicating the Presence of a Small amount of water absorbed in the sample. The band occurring is due to the OH bending of water. The absorption band located is due to asymmetric stretching of the Carbonyl (c=o) group. The peak signifies the existence of the Cu=0 bond. FTIR spectra exist the evidence to observe in-plane and out-of-plane segmental vibration of atoms and molecules with related energies in the IR region. The stretching, bending and bonding can be recognized through FTIR analysis. For example, in CuS, the atoms of Cu are situated at the centre of the hexagonal and sulfide atoms are at the vertices, thus forming a Cu-S-Cu. In our work, Cu-S and Cu-S-Cu fundamental vibrations are found. Figure5(a) the characteristic band at 3330 cm^{-1} corresponds to the vibration mode of water (OH group), indicating the Presence of the small amount of water absorbed on the sample. On the other hand, the band occurring at 3085 cm^{-1} is due to the OH bending of water. The absorption band located at 1146 cm^{-1} is due to the asymmetric stretching of the carbonyl (C=O) group. The peaks at 805 signify the existence of the Cu-O bond. Figure5(b) the characteristic band at 1100 cm^{-1} corresponds to the vibration mode of water (OH group), indicating the Presence of the small amount of water absorbed on the sample. The absorption band located at 772 cm^{-1} is due to the asymmetric stretching of the carbonyl (C=O) group. The peaks at 610 signify the existence of the Cu-O bond. From previous studies, CuS NPs had antibacterial activity against *Staphylococcus aureus* and *Escherichia coli*. Moreover, they could decrease the incidence of bacterial colonization and promote wound healing through re-epithelialization and collagen deposition[19]. The copper-ferrite nanomaterial incorporates catalytic therapy with photothermal therapy to combat bacterial infection, paving a new way for developing antibacterial agents with high synergistic therapeutic outcomes[20]. Furthermore, the combined heterogeneous-homogeneous mechanisms were highly efficient in selectively killing cancer cells due to their GSH levels compared to healthy cell lines[21]. Hydrothermal methods synthesized the pure CuS and CuFeS nanoparticles. The XRD stated the synthesized nanoparticles possess a hexagonal unit cell structure. The FESEM analysis showed synthesized nanoparticles to be hexagonal. The elemental content of the

samples is determined by EDAX analysis. The UV-Visible spectra were analyzed, and the peaks of FTIR spectra were assigned to different pulsation bonds.

4. AUTHORS CONTRIBUTION STATEMENT

L.Thilagavathi and Dr.M. Venkatachalam conceived the presented idea, developed the theory and performed the computations. All others, Dr M Venkatachalam, Dr M.Saroja and Dr T.S.Senthil, verified the materials methods of preparation, encouraged to investigate and supervised the findings of this work. Finally, all authors discussed the results and contributed to the final manuscript.

5. CONFLICT OF INTEREST

Conflict of interest declared none.

6. REFERENCES

1. Podili S, Geetha D, Ramesh PS. Preparation and characterization of porous Hollow Sphere of Ni Doped CuS nanostructures for Electrochemical Supercapacitor Electrode Material. Springer Proc Phys. 2017;189:277-88. doi: 10.1007/978-3-319-44890-9_26.
2. Kong Y, Hou Z, Zhou L, Zhang P, Ouyang Y, Wang P et al. Injectable self-healing hydrogels containing CuS nanoparticles with abilities of hemostasis, antibacterial activity, and promoting wound healing. ACS Biomater Sci Eng. 2021;7(1):335-49. doi: 10.1021/acsbiomaterials.0c01473, PMID 33371671.
3. kong Y, Hou Z, Zhou Liangqin, Zhang Panfeng, Ouyang Yaowen, Wang P et al. Injectable self-healing hydrogels containing CuS nanoparticles with abilities of hemostasis, antibacterial activity, and promoting wound healing. ACS Biomater Sci Eng. 2021;7(1):335-49. doi: 10.1021/acsbiomaterials.0c01473, PMID 33371671.
4. Liang D, Li J, Pang G. A degradation column for organic dyes based on a composite of $CuFeS_2$ nanorystals and sawdust. J Mater Sci.,DOI:10.1007/s10853-016-9844-4.
5. Saranya M, Ramachandran R, Samuel EJJ, Jeong SK, Grace AN. Enhanced visible light photocatalytic reduction of organic pollutant and electrochemical properties of CuS catalyst. Powder Technology. 2015;279:209-20. doi: 10.1016/j.powtec.2015.03.041.
6. Goel S, Chen F, Cai W. Synthesis and biomedical applications of copper sulfide nanoparticles: from sensors to theranostics. Small. 2014 Feb;10(4):631-45. doi: 10.1002/smll.201301174, PMID 24106015.
7. Cardoso J, GomezDaza O, Ixtlilco L, Nair MTS, Nair PK. Conductive copper sulfide thin films on polyimide foils. Semicond Sci Technol. 2001 Feb 1;16(2):123-7. doi: 10.1088/0268-1242/16/2/311.
8. Rajkanan K. Preparation and characterization of thin copper sulfide films for their application in solar cells [doctoral dissertation].
9. Qiu P, Shi X, Chen L. Cu-based thermoelectric materials. Energy Storage Mater. 2016 Apr 1;3:85-97. doi: 10.1016/j.ensm.2016.01.009.
10. Shamraiz U, Hussain RA, Badshah A. Fabrication and applications of copper sulfide (CuS) nanostructures. J Solid State Chem. 2016 Jun 1;238:25-40. doi: 10.1016/j.jssc.2016.02.046.
11. Liu Y, Ji M, Wang P. Recent advances in small copper sulfide nanoparticles for molecular imaging and tumor therapy. Mol Pharm. 2019 Jun 25;16(8):3322-32. doi: 10.1021/acs.molpharmaceut.9b00273, PMID 31287708.
12. Horiuchi Y, Yamashita H. Design of mesoporous silica thin films containing single-site photocatalysts and their applications to superhydrophilic materials. Appl Cat A. 2011 Jun 30;400(1-2):1-8. doi: 10.1016/j.apcata.2011.04.027.
13. Shi L, Wang W, Wu C, Ding J, Li Q. Synthesis of Cu_2SnS_3 nanosheets as an anode material for sodium ion batteries. J Alloys Compd.
14. Liang D, Li J, Pang G. A degradation column for organic dyes based on a composite of $CuFeS_2$ nanorystals and sawdust. J Mater Sci.,DOI:10.1007/s10853-016-9844-4.
15. Alghoraibi I, Zein R. Silver nanoparticles: advances in research and applications is approaching. Silver nanoparticles: advances in research and applications Edwards B, editor; 2017.
16. Harada K. Lorentz microscopy observation of vortices in high- T c superconductors using a 1-MV field emission transmission electron microscope. Microscopy. 2013 Jun 1;62(suppl 1)(suppl_1):S3-15:S3-S15. doi: 10.1093/jmicro/dft013.
17. Wang ZL, Poncharal P, de Heer WA WA. Nanomeasurements in transmission electron microscopy. Microsc Microanal. 2000 May;6(3):224-30. doi: 10.1007/s1000599100023, PMID 10790491.
18. Attal S, Thiruvengadathan R, Regev O. Determination of the concentration of single-walled carbon nanotubes in aqueous dispersions using UV-visible absorption spectroscopy. Anal Chem. 2006 Dec 1;78(23):8098-104. doi: 10.1021/ac060990s, PMID 17134145.
19. Liang Y, Zhang J, Quan H, Zhang P, Xu K, He J et al. Antibacterial effect of copper sulfide nanoparticles on infected wound healing. Surg Infect. 2021 Nov 1;22(9):894-902. doi: 10.1089/sur.2020.411, PMID 33887157.
20. Liu Y, Guo Z, Li F, Xiao Y, Zhang Y, Bu T et al. Multifunctional magnetic copper ferrite nanoparticles as Fenton-like reaction and near-infrared photothermal agents for synergetic antibacterial therapy. ACS Appl Mater Interfaces. 2019 Aug 13;11(35):31649-60. doi: 10.1021/acsami.9b10096, PMID 31407880.
21. Ahamed M, Akhtar MJ, Alhadlaq HA, Alshamsan A. Copper ferrite nanoparticle-induced cytotoxicity and oxidative stress in human breast cancer MCF-7 cells. Colloids Surf B Biointerfaces. 2016 Jun 1;142:46-54. doi: 10.1016/j.colsurfb.2016.02.043, PMID 26925725.
22. Mukhopadhyay R, Kazi J, Debnath MC. Synthesis and characterization of copper nanoparticles stabilized with Quisqualis indica extract: evaluation of its cytotoxicity and apoptosis in B16F10 melanoma cells. Biomed Pharmacother. 2018 Jan 1;97:1373-85. doi: 10.1016/j.biopha.2017.10.167, PMID 29156527.
23. Saranyaadevi K, Subha V, Ravindran RE, Renganathan S. Synthesis and characterization of copper nanoparticle using Capparis zeylanica leaf extract. Int J Chem Tech Res. 2014;6(10):4533-41.